Supporting Information

An enhanced strategy based on the pyrolysis of bean dregs for efficient selective recovery of lithium from spent lithium-ion batteries

Tianning Lin,[a] Yue Wang,[b] Shan Jin,[a] Deying Mu,[a] Jian Zhang,[b] Jianquan Liang,[b] Changsong Dai*[a]

[a] MIIT Key Laboratory of Critical Materials Technology for New Energy Conversion and Storage, School of Chemistry and Chemical Engineering, Harbin Institute of Technology, Harbin 150001, P.R. China

[b] Electric Power Research Institute, State Grid Heilongjiang Electric Power Co., Ltd, Harbin, 150030, P. R. China

Table S1

Elementary contents of bean dregs

Element	C	H	O	N
Wt.%	48.17	6.69	36.62	8.08

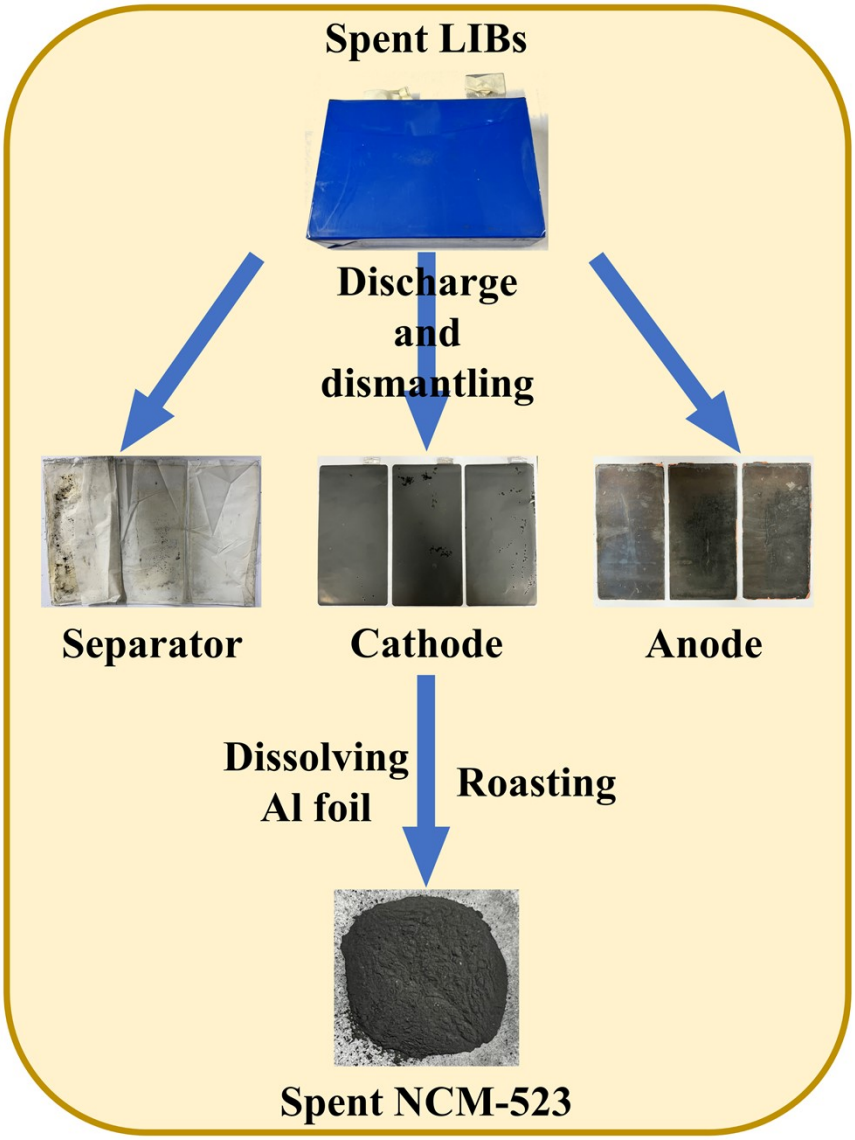

Fig. S1. Pretreatment process of the spent NCM-523 cathode materials.

Table S2

Contents of major elements in SNCM-523.

Element	Li	Ni	Co	Mn	Cu	Al
Wt.%	7.4	32.96	12.72	17.55	0.064	0.107

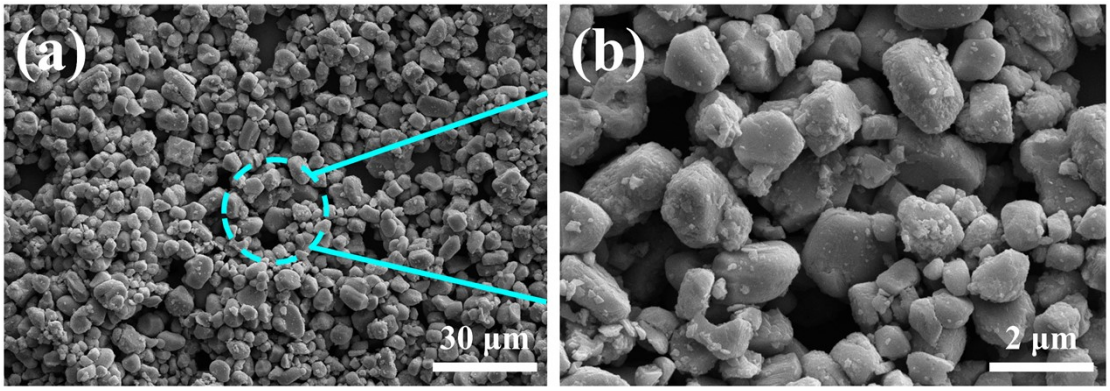

Fig. S2. The SEM images of SNCM-523.

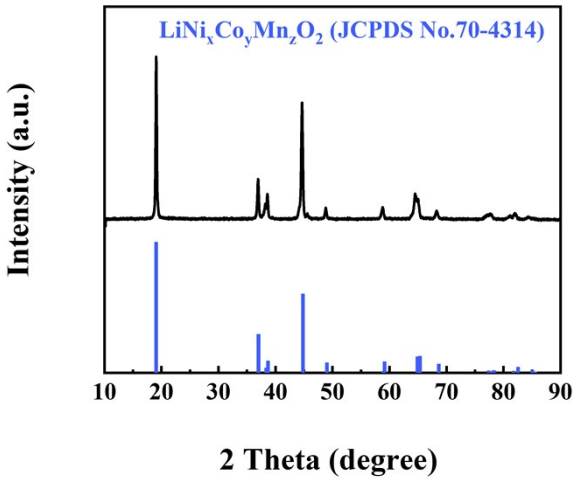

Fig. S3. The XRD pattern of SNCM-523.

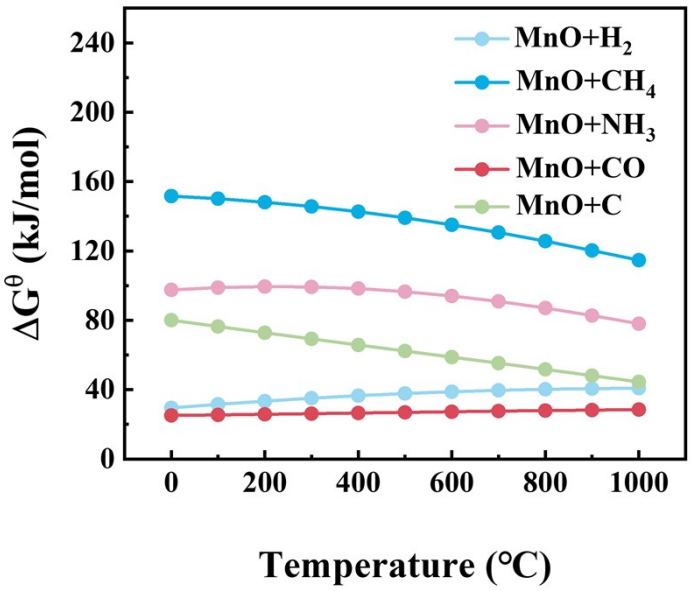

Fig. S4. Schematic diagrams of relationships between the Gibbs free energies and reaction temperatures for the reactions of MnO with reducing gases and biochar.

The reaction formulas of thermal reduction of MnO:

$MnO + H_2 = Mn + H_2O\#(R-S1)$

$4MnO + CH_4 = 4Mn + CO_2 + 2H_2O\#(R-S2)$

$3MnO + 2NH_3 = 3Mn + 3H_2O + N_2\#(R-S3)$

$MnO + CO = Mn + CO_2\#(R-S4)$

$2MnO + C = 2Mn + CO_2\#\ (R-S5)$

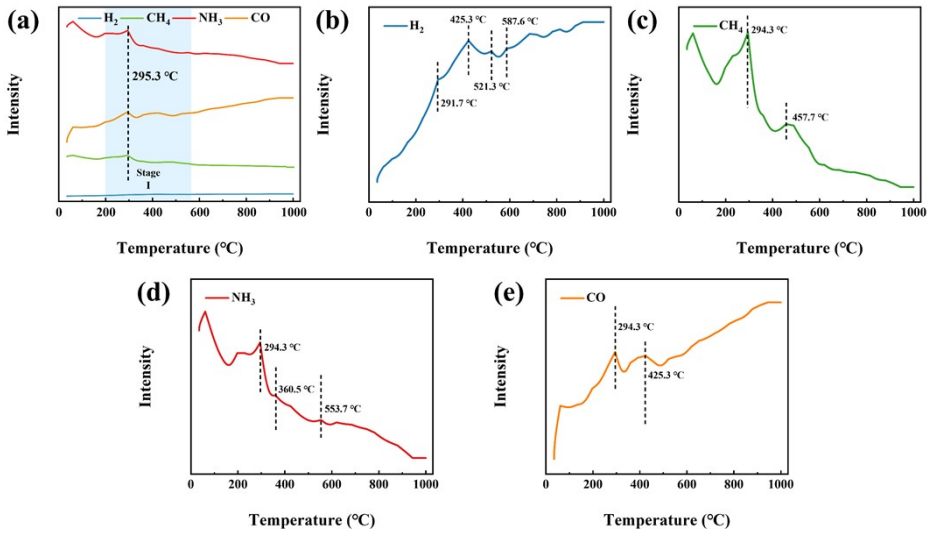

Fig. S5. The mass spectrums of gases produced during roasting process of BDs: (a) main reducing gases, (b) H_2 (m/z = 2), (c) CH_4 (m/z = 16), (d) NH_3 (m/z = 17), and (e) CO (m/z = 28).

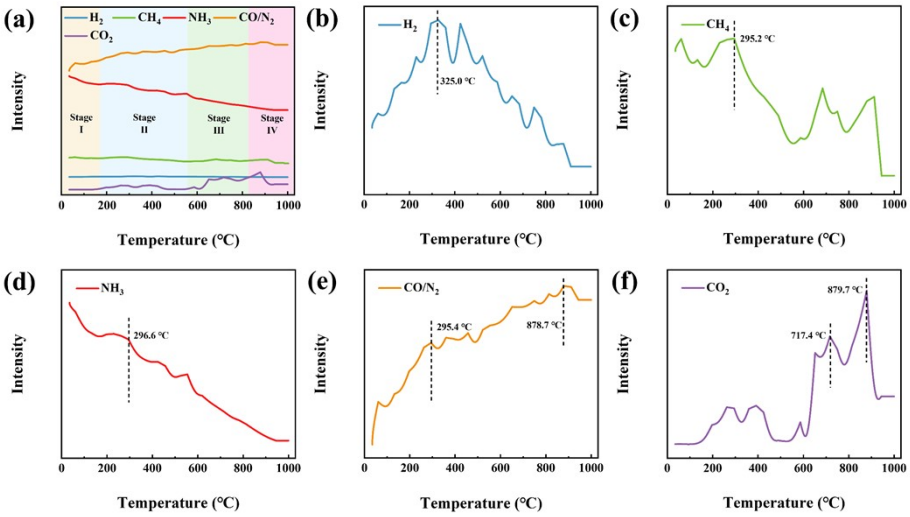

Fig. S6. The mass spectrums of gases produced during roasting process of the mixed samples of BDs and NCM-523: (a) main reducing gases, (b) H_2 (m/z = 2), (c) CH_4 (m/z = 16), (d) NH_3 (m/z = 17), (e) CO/N_2 (m/z = 28), and (f) CO_2 (m/z = 44).

The reason why the mass spectrum of CO is different from other gases is that the m/z of CO is the same as N_2, and N_2 is continuously generated with the reduction reaction of NH_3 and transition metal oxides, so the mass spectrum intensity of CO/N_2 is gradually enhanced.

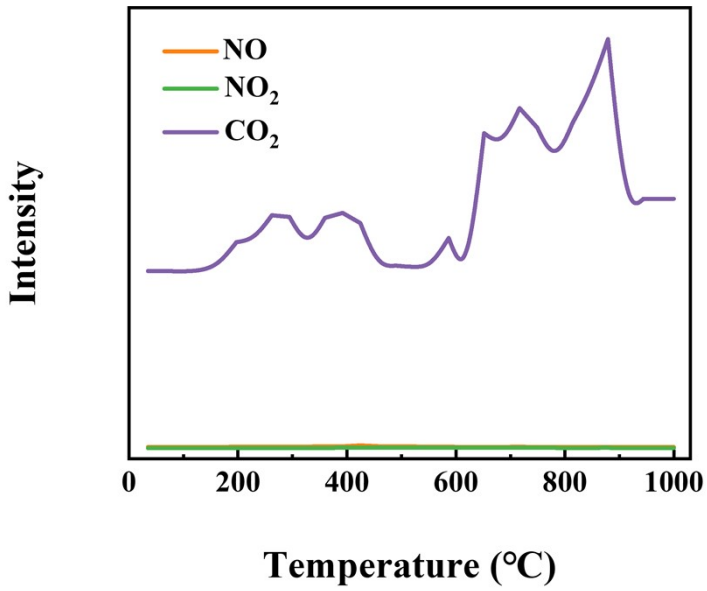

Fig. S7. The mass spectrum of NO, NO_2, and CO_2 produced during roasting process of the mixed samples of BDs and NCM-523.

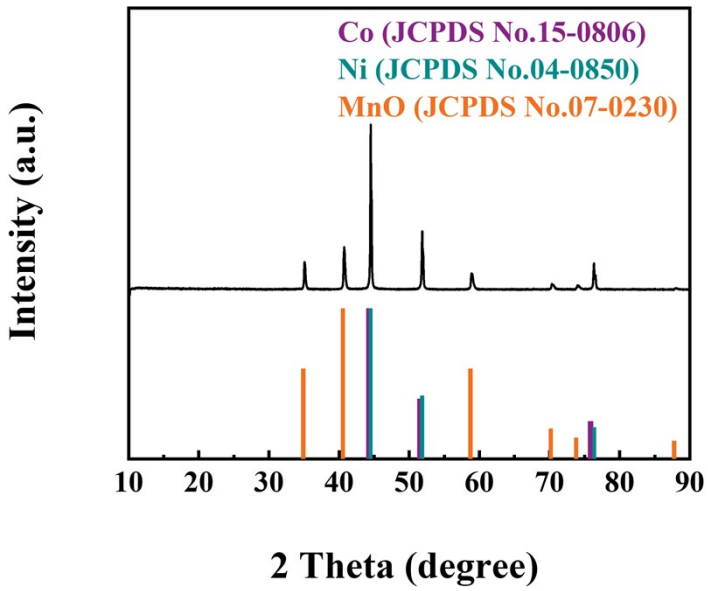

Fig. S8. The XRD pattern of the products after roasting process of BDs and NCM-523 mixed samples (roasting conditions: roasting temperature of 700 ℃, dosage ratio of BDs/NCM-523 of 1:0.5 and roasting time of 1 h).

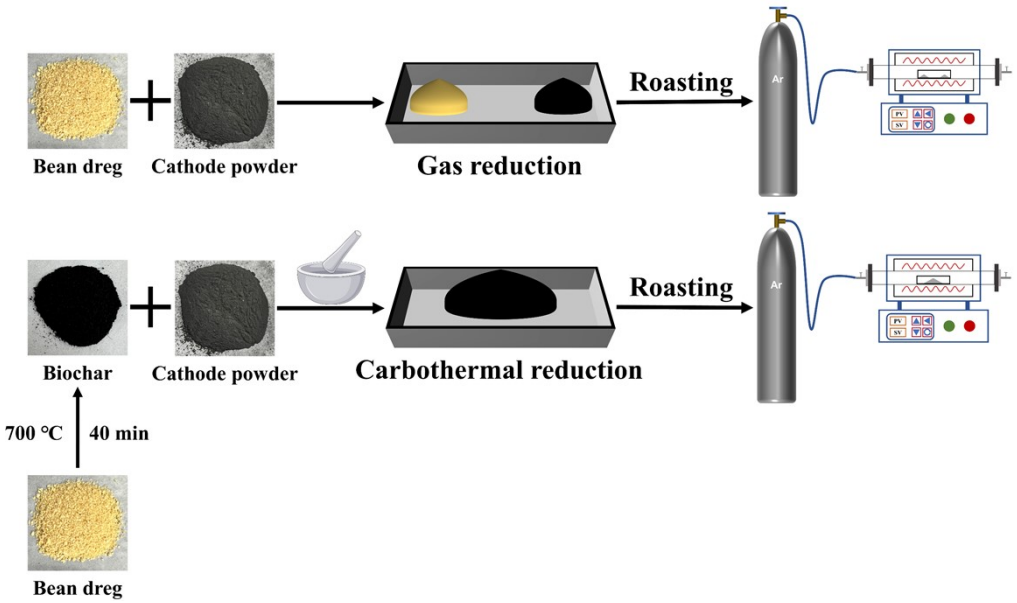

Fig. S9. Schematic diagram of independent exploration of gas reduction and carbothermal reduction.

Experimental procedure

Gas reduction: the BDs and the NCM-523 with the same dosage ratio (1:0.3) as the mixed sample were separated and placed at both ends of the corundum boat, and the BDs were placed in the upper flow of the gas, and then roasted under the same conditions (the roasting conditions: roasting temperature of 700 ℃, dosage ratio of 1:0.3, roasting time of 40 min).

Carbothermal reduction: firstly, the BDs were carbonized in a tube furnace under the conditions of the roasting temperature of 700 ℃ and the roasting time of 40 min. Secondly, the obtained biochar was mixed with NCM-523 in an agate mortar for 10 min, and then transferred to a tube furnace for roasting again with the same conditions (the roasting conditions: roasting temperature of 700 ℃, dosage ratio of 1:0.3, roasting time of 40min).

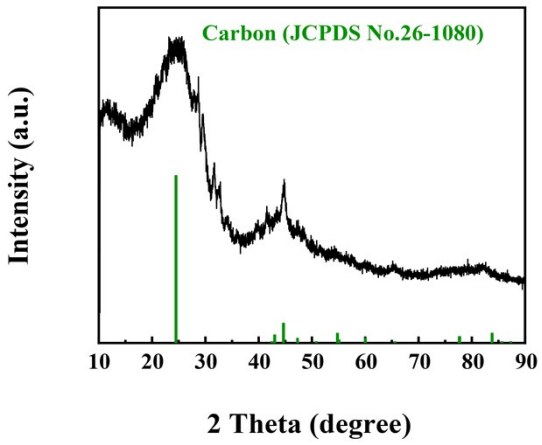

Fig. S10. The XRD pattern of the biochar (the biochar is derived from roasting BDs under optimal roasting conditions).

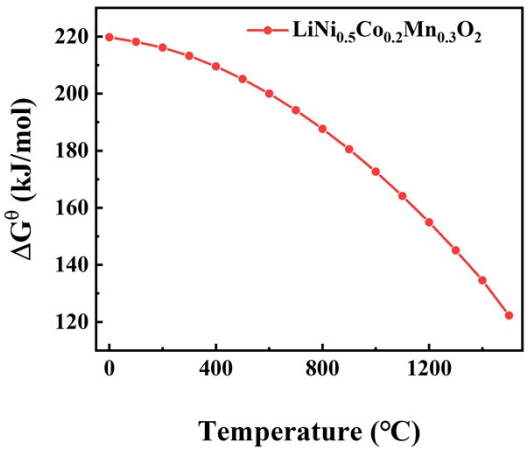

Fig. S11. Schematic diagram of relationship between the Gibbs free energy and reaction temperature of the decomposition reaction of $LiNi_{0.5}Co_{0.2}Mn_{0.3}O_2$.

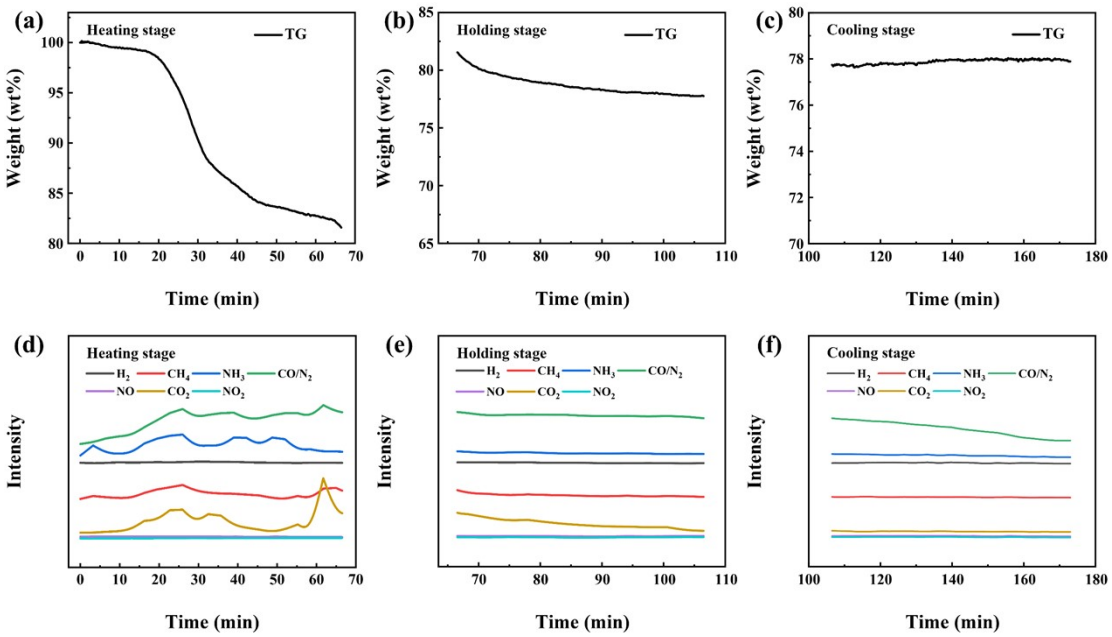

Fig. S12. TG curves and gas mass spectrums of (a) heating stage, (b) holding stage, and (c) cooling stage of the mixed samples (BDs and NCM-523) in Ar atmosphere (dosage ratio: 1:0.3, temperature range: 30-700 ℃, and heating rate: 10 ℃/min).

It can be discovered from Fig. S12, the roasting process can be divided into three stages: heating stage, holding stage, and cooling stage. In the heating stage, the mass spectrum intensities of reducing gases (H_2, CH_4, NH_3, and CO) first increased and then decreased at around 300°C, indicating that gas reduction reactions began to occur. This is also demonstrated by the rising intensity of CO_2. Therefore, in the heating stage, the main off-gas compositions are H_2, CH_4, NH_3, CO, N_2, and CO_2. The mass spectrum intensities of reducing gases and CO_2 continued to decrease in the holding stage, indicating the continuation of reduction reactions and the formation of Li_2CO_3. As a result, the main off-gas compositions are H_2, CH_4, NH_3, CO, N_2, and CO_2 in the holding stage, which is the same as the heating stage. In the cooling stage, with the end of

roasting process, the reduction reactions also tend to be complete. Among them, the intensity of CO_2 is almost negligible, but there are still some unreacted reducing gases (H_2, CH_4, NH_3, and CO) in the off-gas. In conclusion, throughout the whole roasting process, the off-gas compositions can be divided into two parts: 1. the gases generated by the reduction reactions of the NCM-523 decomposition products and the carbon combustion reactions (CO_2, CO, and N_2); 2. the unreacted reduction gases (H_2, CH_4, NH_3, and CO). And Fig. 7 (page 7) have been revised to insert the off-gas, which is attached below for your convenience. At the same time, in both Fig. S12 and Fig. S7, extremely low mass spectrum intensities of NO and NO_2 indicate there is no NO and NO_2 in the off-gas which are harmful to the environment and may cause acid rain.

Optimization of carbonated water leaching

Model construction and verification

Among the many response surface methods, the CCD is comparatively better because of larger operability area.[1] Simultaneously, the CCD enables accurate prediction of center points and is insensitive to any missing data points.[2,3] Herein, the CCD method was chosen to design the carbonated water leaching process in this study. It is acknowledged from previous research works that leaching time (h), CO_2 flow rate (mL/min), temperature (℃) and solid-liquid ratio (g/L) are the main parameters which affecting the leaching rate of Li. Hence, taking the four parameters as the main influencing factors, the corresponding response value is the leaching rate of Li. Five-level coding factors were exploited for the experimental design, and the corresponding values are listed in Table S3. On the foundation of the previous research works on the single-factor exploration results of the carbonated water leaching process, the factor range of the experiment initial design was determined.[4] There are 31 groups of experimental design matrices, including 16 factorial points, 7 center points, and 9 axial points, respectively, and the obtained design matrix and the actual values of all responses are demonstrated in Table S4. Additionally, regression analysis was performed on the experimental data by RSM, and the fitted second-order polynomial equation model equations were presented in Eq. S1.

So as to determine the suitability of the selected model, statistical analysis of the obtained experimental data was performed by analysis of variance (ANOVA).[5]

ANOVA was also used to measure the significance of each independent factor, goodness of fit, lack of fit, Fisher's test (F-value), and probability (p-value).[6] The results of ANOVA are presented in Table S5. From the ANOVA results table, the F-test is utilized to determine the significance of the variables influence in the regression equation on leaching rate of Li, and the significance of variables is usually tested by the p-value, which can also reflect the strength of the interaction between independent variables. The smaller the probability of p, the higher the significance of the corresponding variable, and the better the significance effect. The F value obtained by the Fisher's test is 28.12, and the p-values are less than 0.05, therefore, the constructed quadratic regression model can be considered sufficient. The coefficients of the quadratic regression model design Eq. S1 were determined by multiple regression analysis. The positive and negative signs in front of the model term indicate the synergistic and antagonistic effects of the factor on the response, respectively.

$$\begin{aligned} Y(\mathrm{Li}) = {} & 95.79 + 0.1879A + 0.2837B + 0.6537C - 1.11D - 0.0606AB \\ & + 0.0056AC + 0.0844AD + 0.0644BC - 0.0194BD + 0.1844CD \\ & - 0.2867A^2 - 0.2467B^2 - 0.2205C^2 - 0.4105D^2 \end{aligned} \quad (4)$$

The coefficient of determination (R^2) (representing experimental proximity) and the Adeq Precision in Table S6 were used to determine the goodness of fit.[4] A larger R^2 value indicates better model importance and response predictability. The R^2 value in this study was 0.96, indicating that the model explained 96% of the experimental data excellently. In addition, if the difference between predicted R^2 and adjusted R^2 is less

than 0.2, it can be considered that the model fits nicely. According to the values of predicted R^2 and adjusted R^2 in Table S4, the difference between them is less than 0.2, only 0.08, revealing that the model is desirably fitted. Then, as shown in Fig. S12, most of the data points are symmetrically scattered around the diagonal line that implies that the actual and predicted values are equal under ideal conditions, implying that the experimental results are in good agreement with the predicted values, which verifies the higher R^2 value of the model. At the same time, with the intention of better predicting the model, the Adeq Precision which denoting that the range of the expected response in relation to its connection error should be greater than 4. In the model, the Adeq Precision value of 18.7 is well above the limit of the response, indicating that the model is nicely predicted. Besides, the accuracy of model can also be represented by C.V. in Table S6. The smaller the value of C.V. (0.38), the better the fit and the higher the reliability of the experiment. Therefore, the model can be utilized to analyze and predict the carbonated water leaching process to optimize leaching conditions.

Table S3

Selected factors with their corresponding levels.

Coded value	A: Time	B: Flow rate	C: Temperature	D: Solid-liquid ratio
-2	1	0	20	10
-1	2	50	35	15
0	3	100	50	20
1	4	150	65	25
2	5	200	80	30

Table S4

Design and results of response surface method.

		Factor 1	Factor 2	Factor 3	Factor 4	Response 1
Std	**Run**	**A: Time**	**B: Flow rate**	**C: Temperature**	**D: Solid-liquid ratio**	**Leaching rate of Li**
		h	**mL/min**	**℃**	**g/L**	**%**
1	16	2	50	35	25	95.16
2	2	4	50	35	25	95.22
3	28	2	150	35	25	95.43
4	30	4	150	35	25	95.44
5	22	2	50	65	25	95.53
6	3	4	50	65	25	95.89
7	9	2	150	65	25	96.38
8	17	4	150	65	25	96.33
9	21	2	50	35	35	92.38
10	31	4	50	35	35	93.01
11	20	2	150	35	35	92.85
12	26	4	150	35	35	93.16
13	19	2	50	65	35	93.85
14	24	4	50	65	35	94.34
15	1	2	150	65	35	94.37
16	23	4	150	65	35	94.67
17	4	1	100	50	30	94.03
18	5	5	100	50	30	95.23
19	8	3	0	50	30	93.9
20	25	3	200	50	30	95.68

21	18	3	100	20	30	93.15
22	12	3	100	80	30	96.64
23	15	3	100	50	20	96.58
24	7	3	100	50	40	91.69
25	29	3	100	50	30	95.82
26	6	3	100	50	30	95.99
27	10	3	100	50	30	94.97
28	13	3	100	50	30	95.85
29	27	3	100	50	30	95.97
30	11	3	100	50	30	96.07
31	14	3	100	50	30	95.83

Table S5

ANOVA for response surface quadratic model for leaching rate of Li.

Source	Sum of Squares	df	Mean Square	F-value	p-value	
Model	51.18	14	3.66	28.12	< 0.0001	**significant**
A-A	0.8475	1	0.8475	6.52	0.0213	
B-B	1.93	1	1.93	14.87	0.0014	
C-C	10.26	1	10.26	78.91	< 0.0001	
D-D	29.33	1	29.33	225.60	< 0.0001	
AB	0.0588	1	0.0588	0.4524	0.5108	
AC	0.0005	1	0.0005	0.0039	0.9510	
AD	0.1139	1	0.1139	0.8763	0.3631	
BC	0.0663	1	0.0663	0.5101	0.4854	
BD	0.0060	1	0.0060	0.0462	0.8325	
CD	0.5439	1	0.5439	4.18	0.0576	
A^2	2.35	1	2.35	18.09	0.0006	
B^2	1.74	1	1.74	13.39	0.0021	
C^2	1.39	1	1.39	10.69	0.0048	
D^2	4.82	1	4.82	37.07	< 0.0001	
Residual	2.08	16	0.1300			
Lack of Fit	1.25	10	0.1251	0.9050	0.5772	**not significant**
Pure Error	0.8292	6	0.1382			
Cor Total	53.26	30				

Table S6

Fit Statistics.

Std. Dev.	0.3605	**R^2**	0.9609
Mean	94.88	**Adjusted R^2**	0.9268
C.V. %	0.3800	**Predicted R^2**	0.8436
		Adeq Precision	18.6572

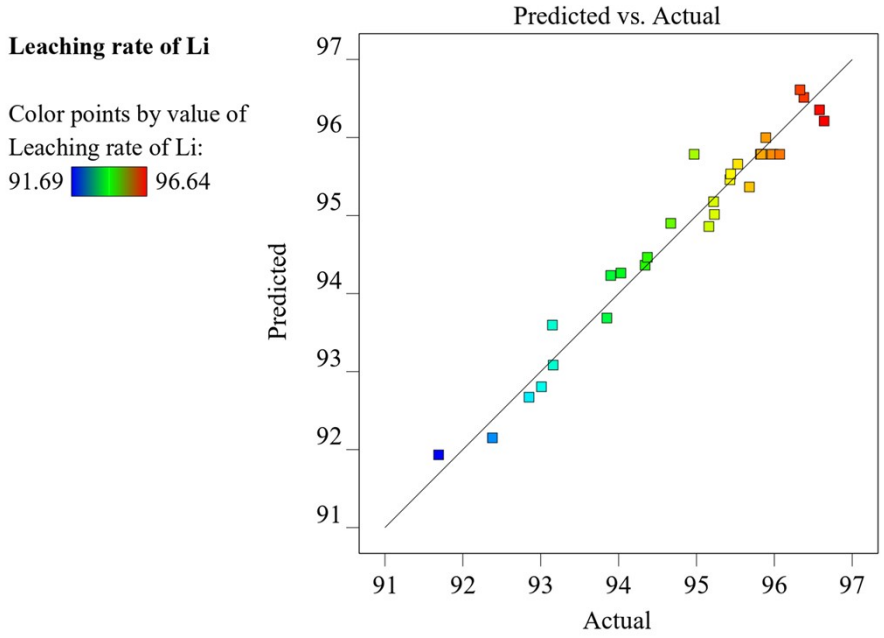

Fig. S13. Plot of CCD predictions and response variable measured values of Li leaching rate.

The diagnostic diagram of the experimental value and the model predicted value, the data blocks drawn in different colors in the diagram represent the efficiency, and the color points are distributed according to the response value, and the order is blue, green, yellow, and red, where red represents the largest response value.

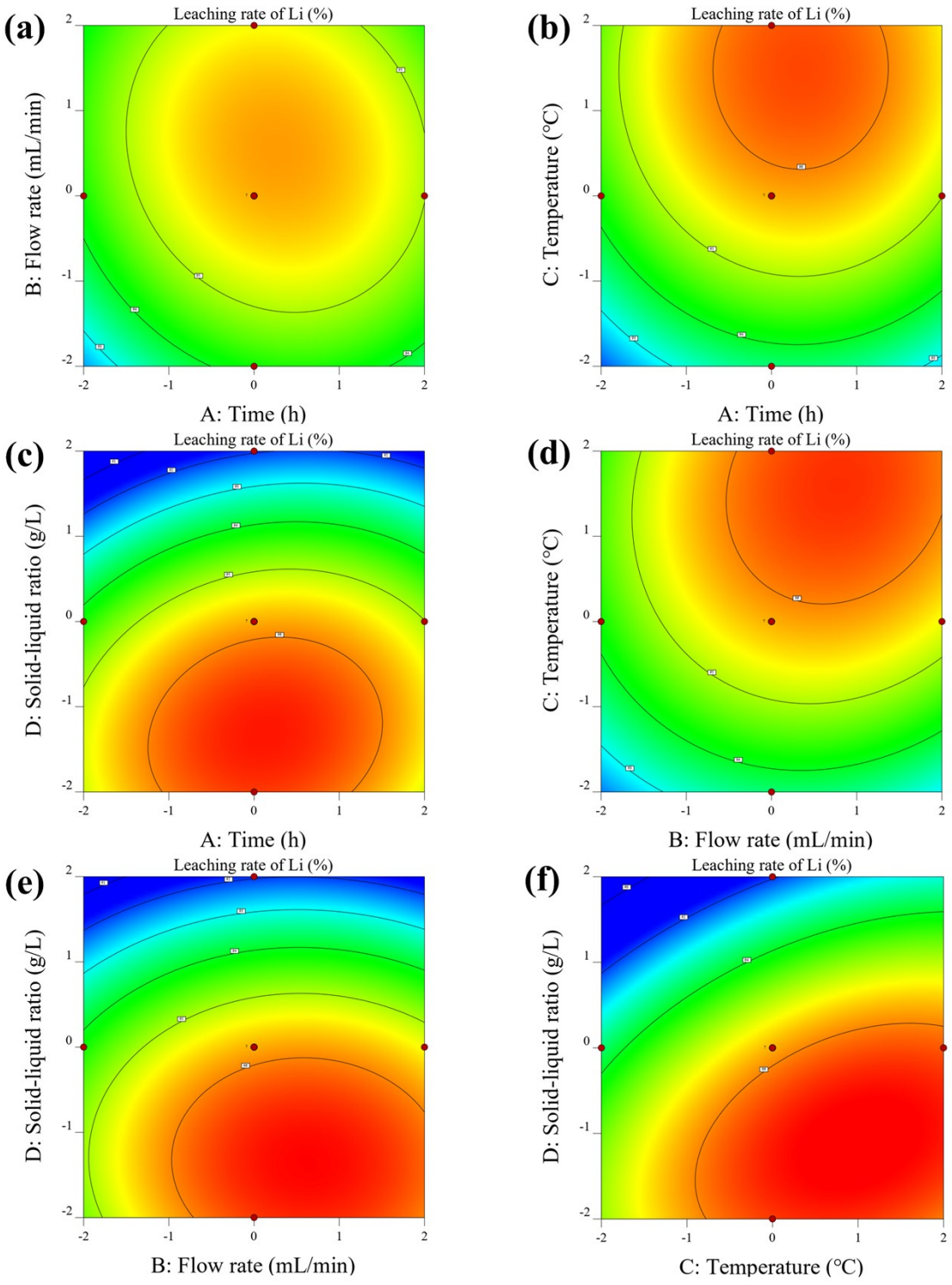

Fig. S14. 2D contour plots of the response surface analysis: (a) time and flow rate, (b) time and temperature, (c) time and solid-liquid ratio, (d) flow rate and temperature, (e) flow rate and solid-liquid ratio, and (f) temperature and solid-liquid ratio.

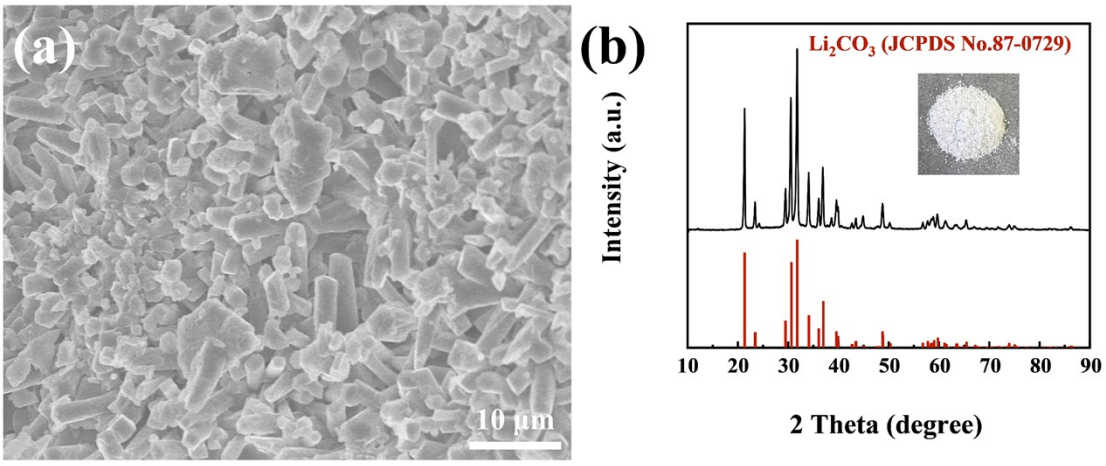

Fig. S15. The SEM image and the XRD pattern for the recovered Li_2CO_3.

Table S7

Chemical composition of the recovered Li_2CO_3.

Composition	Li_2CO_3	Ni	Co	Mn	Cu	Al
Mass (%)	>99.79	0.073	0.021	0.054	0.048	0.016

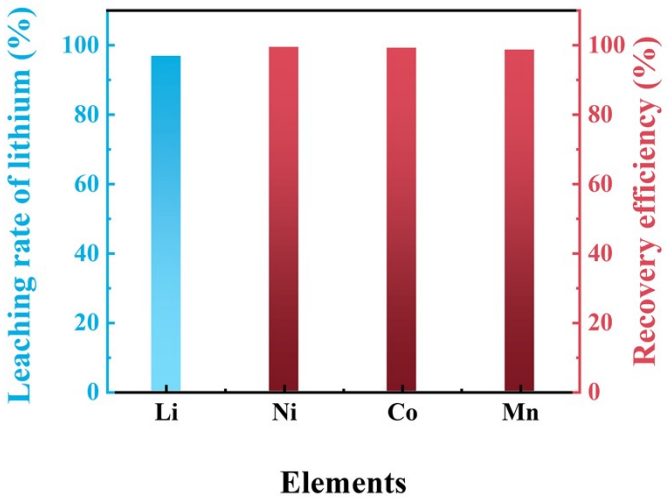

Fig. S16. The leaching rate of Li and the recovery efficiencies of Ni, Co, and Mn after biomass reduction roasting and carbonated water leaching.

Economic assessment

The enhanced recycling strategy designed in this study is mainly divided into three parts: roasting; leaching, filtration, and evaporation; magnetic separation. It is assumed that 1 ton of spent NCM-523 is processed in China through the designed recycling process. The spent NCM-523 cathode material powder is obtained from a specialized spent LIBs collection and recycling company, which the cost is calculated at \$197.26/ton (the cost of collection and transportation, $C_{C\&T}$). For the labor costs, the working day is 300 days per year (an average of 25 days per month), while the working hours are approximately 8 hours per day. The per capita wage in China is 74,318 yuan per year (\$37 per day, \$1 = 6.75 yuan). The industrial electricity charge is \$0.20/kWh (max), the industrial water charge is \$0.40/t (max), and the industrial liquid CO_2 price is \$14.81/40 L. The price of BDs is \$150/t (p_B) .[7]

Considering the residual rate and interest rate, the depreciation cost of equipment is calculated as Eq. (S2) and the formula for calculating equipment maintenance cost is Eq. (S3):

$$C_D = C_0 \times (1 - r) \times \frac{i}{1 - (1 + i)^{-n}} \#(S2)$$

C_D — — — Depreciation cost of equipment

C_0 — — — Acquisition cost of equipment

r — — — Residuals rate of equipment, 4%

i — — — Interest rate, 10%

n — — — Service life, year

$$M_c = 0.05 \times C_0 \#(S3)$$

M_C — — — Maintenance cost of equipment

C_0 — — — Acquisition cost of equipment

And the energy consumption, the cost of electric power, water and labor are calculated as Eq. (S4), (S5), and (S6):

$$C_p = P \times t \times n \times p_e \#(S4)$$

C_P — — — Cost of electric power

P — — — Equipment power, Kw

t — — — Working time of equipment

n — — — Number of equipments

p_e — — — Electricity price for industrial uses, \$0.20/kWh

$$C_w = m \times p_w \#(S5)$$

C_w — — — Cost of water

m — — — Water consumption, ton

p_w — — — Water price for industrial uses, \$0.91/t

$$C_l = n \times p_l \#(S6)$$

C_l — — — Cost of labor

n — — — Number of workers

p_l — — — Wage of per labor, \$39/day

Finally, the energy consumption and cost of each process in this study and the benefits of gaining products are calculated in detail, and then the profit of recycling 1

ton of spent NCM-523 cathode material according to the designed recycling process in China is attained.

Process I: Reduction roasting

Requirement: Two heating equipment (P_w = 55 kW, per price = \$216000, maximum capacity = 350 kg/per, service life = 5 years) are needed to respectively work for 4h every day. In this recycling process, the obtained mixed cathode materials were roasted, which means every device needs to work 2 times every day.

Electric power charge: the working time including temperature rise and hold is 2 h and the cooling time is 0.5-1 h.

$$C_D = C_0 \times (1 - r) \times \frac{i}{1 - (1 + i)^{-n}}$$

$$C_D = (\$216000 \times 2 \times \frac{1}{300}) \times (1 - 4\%) \times \frac{10\%}{1 - (1 + 10\%)^{-5}} = \$365$$

$$M_c = 0.05 \times C_0$$

$$M_c = 0.05 \times (\$216000 \times 2 \times \frac{1}{300}) = \$72$$

$$C_p = P \times t \times n \times p_e$$

$$C_p = 55\ \text{kW} \times 2.5\ \text{h} \times 2 \times \$0.20/\text{kWh} = \$55$$

$$C_l = n \times p_l$$

$$C_l = 1 \times \$37 = \$37$$

$$C_B = n \times p_B$$

$$C_B = 0.3 \times \$150 = \$45$$

Total costs: \$574

After this process, the calcined powders are about 1.04 ton

Process II: Leaching, filtration and evaporation

Requirement: The roasted powder was leached in carbonated water, the conditions

were the time of 3.1 h, the CO_2 flow rate of 135 mL/min, the temperature of 67 ℃, and the solid-liquid ratio of 25 g/L. During the leaching process, four heaters is needed to maintain the temperature (P_w = 15 kW, unit price = \$290, service life = 5 years), and CO_2 is introduced to increase the leaching rate of Li_2CO_3 (the price of liquid CO_2 is \$0.37/L). The supernatant liquor was filtered by four self-discharging filtering machines (P_w = 20 kW, per price = \$5800, maximum capacity = 4 ton/hour, service year = 3 years) while the slurry was bag-type filtered; about 41.6 ton of water is consumed. After the carbonated water leaching process, 96.83% of Li_2CO_3 would dissolve in water and evaporate to obtain about 300 kg of Li_2CO_3 crystals. The filter needs to work about 6 hours a day. The leachate uses mechanical evaporation to evaporate water to recover Li_2CO_3, which is realized by two multi-stage evaporators (P_w = 48 kW, unit price = \$72,000, maximum capacity = 7 tons/hour, service life = 5 years), while the second one is naturally evaporated.

Leaching and filtering:

$$C_{D1} = C_0 \times (1 - r) \times \frac{i}{1 - (1 + i)^{-n}}$$

$$C_{D1} = (\$290 \times 4 \times \frac{1}{300}) \times (1 - 4\%) \times \frac{10\%}{1 - (1 + 10\%)^{-5}} = \$0.98$$

$$C_{D2} = C_0 \times (1 - r) \times \frac{i}{1 - (1 + i)^{-n}}$$

$$C_{D2} = (\$5800 \times 4 \times \frac{1}{300}) \times (1 - 4\%) \times \frac{10\%}{1 - (1 + 10\%)^{-5}} = \$20$$

$$M_{c1} = 0.05 \times C_0$$

$$M_{c1} = 0.05 \times (\$290 \times 4 \times \frac{1}{300}) = \$0.19$$

$$M_{c2} = 0.05 \times C_0$$

$$M_{c2} = 0.05 \times (\$5800 \times 4 \times \frac{1}{300}) = \$4$$

$$C_{p1} = P \times t \times n \times p_e$$

$$C_{p1} = 15\,kW \times 3.1\,h \times 4 \times \$0.20/kWh = \$37.2$$

$$C_{p2} = P \times t \times n \times p_e$$

$$C_{p2} = 55\,kW \times 2.6\,h \times 4 \times \$0.20/kWh = \$114.4$$

$$C_l = n \times p_l$$

$$C_l = 4 \times \$37 = \$148$$

$$C_w = n \times p_w$$

$$C_w = 41.6 \times \$0.4 = \$17$$

Evaporating:

$$C_D = C_0 \times (1 - r) \times \frac{i}{1 - (1 + i)^{-n}}$$

$$C_D = (\$72000 \times \frac{1}{300}) \times (1 - 4\%) \times \frac{10\%}{1 - (1 + 10\%)^{-5}} = \$61$$

$$M_c = 0.05 \times C_0$$

$$M_c = 0.05 \times (\$72000 \times \frac{1}{300}) = \$12$$

$$C_p = P \times t \times n \times p_e$$

$$C_p = 48\,kW \times 6h \times \$0.20/kWh = \$57.6$$

Total costs: $472

After this process, about 71.65 kg of Li_2CO_3 crystals were recovered. Finally, the filter residues are about 675.49 ton.

Process III: Magnetic separation

Requirement: Purification of Ni, Co, and MnO in leaching slag by wet magnetic flotation technology. Purification equipment (P = 40 kW, per price = $36000, maximum capacity = 1 ton/hour, service life = 5 years)

$$C_D = C_0 \times (1 - r) \times \frac{i}{1 - (1 + i)^{-n}}$$

$$C_D = (\$3600 \times \frac{1}{300}) \times (1 - 4\%) \times \frac{10\%}{1 - (1 + 10\%)^{-5}} = \$3$$

$$M_c = 0.05 \times C_0$$

$$M_c = 0.05 \times (\$3600 \times \frac{1}{300}) = \$0.6$$

$$C_p = P \times t \times n \times p_e$$

$$C_p = 40\,\text{kW} \times 1\,\text{h} \times 3 \times \$0.20/\text{kWh} = \$24$$

$$C_l = n \times p_l$$

$$C_l = 0.375 \times \$32 = \$12$$

Total costs: $39.6

After this process, about 326.96 kg of Ni, 126.06 kg of Co, and 174.45 kg of MnO can be recycled.

Therefore, the total costs of whole processes (C_T) in this study can be

$$C_T = \$574 + \$472 + \$42.6 = \$1098.6$$

Table S8

Revenues of products by this recycling process

Product	Daily production (kg)	Prices(/t)	Revenue
Li_2CO_3	71.65	69630	4988.99
Ni	326.96	24741	8089.32
Co	126.06	48889	6162.95
MnO	174.45	741	129.27
Total revenues			19370.53

Thus, the day's profit (P) can be obtained:

$$P = R - C_{C\&T} - C_T = \$19370.53 - \$197.26 - \$1098.6 = \$18074.67$$

To sum up the above, the daily profit of the recycling process designed in this study is $18047.67.

Table S9

The costs, revenues, and profits of the recovery process

Costs	Revenues	Profits
1295.86	19370.53	18074.67

Table S10

Chemical composition of the carbonated water leaching product.

Composition	**Ni-Co-MnO**	**Carbon**	**Li**	**Cu**	**Fe**	**Al**
Mass (%)	97.17	2.28	0.09	0.01	0.18	0.08

From Table S10, after the entire recycling process, the main impurity in the carbonated water leaching product is carbon. Meanwhile, it can be comprehended from the XRD pattern in Fig. S10 that when BDs were roasted alone under the optimized roasting conditions, the remaining solid product is mainly biochar, which also can be recognized in the previous reports.[8,9] Therefore, the thermal-stable and water-insoluble biochar is the main impurity which mixed with transition metals in the solid phase throughout the entire recycling process.

Table S11

A brief comparison of different reduction roasting processes.

Ref.	Type	Reductant	Recovery efficiency of Li (%)	Recovery Profits ($/kg)	Environmental influence
[10]	LCO, LMO, LNO	Anode graphite	92.25	–	CO_2 emissions
[11]	LMO	Anode graphite	81.90	–	CO_2 emissions
[12]	NCM	Anode graphite	90	–	CO_2 emissions
[4]	NCM	Lignite	84	–	CO_2 emissions
[13]	NCM	Lignite	84.7	–	CO_2 emissions
[14]	NCM	Coke	93.67	–	CO_2 emissions
[15]	NCM	Macadamia Shells	93.4	–	Carbon neutral
[8]	LCO	Pine sawdust	94	19.99	Carbon neutral
[9]	LCO	Rice straw	90	–	Carbon neutral
This study	NCM	Bean dregs	96.83	18.07	Carbon neutral

(– indicates that the corresponding reference has no corresponding data)

References

1. L. V. Candioti, M. M. De Zan, M. S. Camara and H. C. Goicoechea, *Talanta*, 2014, **124**, 123-138.
2. S. Madadi, L. Charbonneau, J.-Y. Bergeron and S. Kaliaguine, *Appl. Catal. B-Environ.*, 2020, **260**.
3. A. A. A, S. Mondal, S. M. Pudi, N. N. Pandhare and P. Biswas, *Energy Fuels*, 2017, **31**, 8521-8533.
4. J. Zhang, J. Hu, W. Zhang, Y. Chen and C. Wang, *J. Clean. Prod.*, 2018, **204**, 437-446.
5. M. N. Catrinck, E. S. Ribeiro, R. S. Monteiro, R. M. Ribas, M. H. P. Barbosa and R. F. Teófilo, *Fuel*, 2017, **210**, 67-74.
6. N. Bala, M. Napiah and I. Kamaruddin, *Int. J. Pavement Eng.*, 2018, **21**, 29-40.
7. Y. Yang, X. Meng, H. Cao, X. Lin, C. Liu, Y. Sun, Y. Zhang and Z. Sun, *Green Chem.*, 2018, **20**, 3121-3133.
8. F. Zhou, X. Qu, Y. Wu, J. Zhao, S. Gao, D. Wang and H. Yin, *ACS Sustain. Chem. Eng.*, 2022, **10**, 1287-1297.
9. X. Chen, Y. Wang, S. Li, Y. Jiang, Y. Cao and X. Ma, *Chem. Eng. J.*, 2022, **434**.
10. B. Makuza, D. Yu, Z. Huang, Q. Tian and X. Guo, *Resour. Conserv. Recycl.*, 2021, **174**.
11. J. Xiao, J. Li and Z. Xu, *Environ. Sci. Technol.*, 2017, **51**, 11960-11966.
12. Y. Zheng, P. Shao, L. Yang, Y. Huang, H. Zhang, L. Fang, C. Qiu, H. Tang, J. Shao and X. Luo, *Resour. Conserv. Recycl.*, 2023, **188**.
13. J. Hu, J. Zhang, H. Li, Y. Chen and C. Wang, *J. Power Sources*, 2017, **351**, 192-199.
14. P. Liu, L. Xiao, Y. Tang, Y. Chen, L. Ye and Y. Zhu, *Journal of Thermal Analysis and Calorimetry*, 2018, **136**, 1323-1332.
15. Y. Zhao, B. Liu, L. Zhang and S. Guo, *J. Hazard. Mater.*, 2020, **396**, 122740.